Int J Thermophys (2010) 31:2119–2146
DOI 10.1007/s10765-010-0874-x

Densities, Excess Molar Volumes, Ultrasonic Speeds, and Isentropic Compressibilities of Hexan-1-ol with 1,2-Dichloroethane, 1,2-Dibromoethane, and 1,1,2,2-Tetrachloroethene at (293.15 and 298.15) K

Subhash C. Bhatia · Rachna Bhatia ·
Gyan P. Dubey

Received: 6 October 2008 / Accepted: 3 November 2010 / Published online: 25 November 2010

Abstract Densities, ρ, and ultrasonic speeds, u, of binary mixtures of hexan-1-ol with 1,2-dichloroethane, 1,2-dibromoethane, and 1,1,2,2-tetrachloroethene have been measured over the entire range of composition at (293.15 and 298.15) K and atmospheric pressure. From these data, the excess molar volumes, V^{E}, deviations of ultrasonic speed, u^{D}, from the ultrasonic speed of an ideal mixture, excess molar isentropic compressibilities, $\kappa_{S,\mathrm{m}}^{\mathrm{E}}$, intermolecular free lengths, L_{f}, mean molecular radii, r, and thermal expansion coefficients, α, have been calculated. The experimental ultrasonic speeds have been analyzed in terms of Nomoto's, Van Dael's ideal mixture, and Junjie relations; Jacobson's free length and Schaaffs' collision factor theories; and thermo-acoustical parameters.

Keywords Excess molar volumes · Halohydrocarbons · Hexan-1-ol · Jacobson's free length theory · Schaaffs' collision factor theory

1 Introduction

The mixing of different liquids produces solutions that generally do not behave ideally. The deviation from ideal behavior can be expressed by excess thermodynamic properties of liquid mixtures. In particular, they correspond to the interactions that take place between solute–solute (A–A), solvent–solvent (B–B), and solute–solvent

---

S. C. Bhatia (✉) · R. Bhatia · G. P. Dubey
Department of Chemistry, Kurukshetra University, Kurukshetra 136119, India
e-mail: bhatiasc2@rediffmail.com

R. Bhatia
e-mail: bhatiarachna_3@rediffmail.com

G. P. Dubey
e-mail: gyan.dubey@rediffmail.com

(A–B) species. These properties are quite useful in the study of the nature of molecular interactions in the liquid mixtures [1–5]. The mixture thermodynamic properties obtained from a measurement of density and speed of sound can provide insight into the nature of molecular interactions in liquid mixtures. A literature survey indicates that not much work has been carried out on the study of thermodynamic properties of binary mixtures of halohydrocarbons with higher alkanols. The variations in the volumetric and acoustic properties of binary mixtures of alkanols containing haloalkanes, acetonitrile, ethylacetate, and ethenyl ethanoate, with the molecular size, shape, chain-length, and degree of molecular association of normal alkanols and branched alkanols have been reported earlier [6–19]. Alkanols are polar and self-associated liquids, and the dipolar association of alkanols decreases when they are mixed with polar compounds containing halogen atoms, due to some sort of specific intermolecular interactions between the hydroxyl oxygen of alkanols and the haloalkanes [16–23].

Here, we report experimental results of density, ρ, and ultrasonic speed, u, of binary liquid mixtures of hexan-1-ol with 1,2-dichloroethane (DCE) 1,2-dibromoethane (DBE), and 1,1,2,2-tetrachloroethene (TCE) at 293.15 K and 298.15 K over the entire range of mixture mole fractions. From the experimental values of the density and ultrasonic speed, the excess molar volumes, V^{E}, deviations of ultrasonic speed, u^{D}, from the ultrasonic speed of an ideal mixture, excess molar isentropic compressibilities, $\kappa_{S,\mathrm{m}}^{\mathrm{E}}$, intermolecular free lengths, L_{f}, mean molecular radii, r, and thermal expansion coefficients, α, have been calculated. The experimental ultrasonic speeds have been analyzed in terms of Nomoto's relation (NR), Van Dael's ideal mixture relation (IMR), Jacobson's free length theory (FLT), Junjie relation (JR), Schaaffs' collision factor theory (CFT), and thermoacoustical parameters (TAP).

2 Experimental

2.1 Materials

The mole fraction purities of the liquids from s. d. fine Chemical Ltd., India, were: 1,2-dichloroethane (99.7 %), 1,2-dibromoethane (99.5 %), 1,1,2,2-tetrachloroethene (99.4 %), and hexan-1-ol (99.7 %). Prior to the experimental measurements, all the liquids were stored in dark bottles over 0.4 nm molecular sieves to reduce water content and were partially degassed with a vacuum pump under a nitrogen atmosphere. The purities of all the samples as determined by chromatographic analysis were better than 99.5 % on a molar basis. Density and ultrasonic speed values of the pure liquids and their mixtures at (293.15 and 298.15) K were measured with an Anton Paar digital densimeter (Model DSA 5000, Austria) operated in the static mode and automatically thermostated within ±0.001 K.

The densities have a precision better than $\pm 2 \times 10^{-3}\,\mathrm{kg \cdot m^{-3}}$, and the speeds of sound are accurate to $1\,\mathrm{m \cdot s^{-1}}$. Densities and ultrasonic speeds of the pure liquids were in good agreement with values found in the literature [10,14,17,20,24]; see Table 1.

Table 1 Physical properties of pure liquid components

Pure liquid	T (K)	ρ $(\mathrm{g \cdot cm^{-3}})$		u $(\mathrm{m \cdot s^{-1}})$		α $(\mathrm{kK})^{-1}$	
		Expt	Lit	Expt	Lit	Expt	Lit
Hexan-1-ol	298.15	0.815281	0.815340 [24] 0.815230 [20]	1303.19	1304.72 [20]	0.8753	0.8861 (303.15 K) [20]
1,2-Dichloroethane	298.15	1.245555	1.246370 [24]	1193.60	1174.0 (303.15 K) [17]	1.1579	1.141 (293.15 K) [24]
1,2-Dibromoethane	298.15	2.169137	2.16870 [24]	994.27	993.73 [14]	0.9639	0.964 [14]
1,1,2,2-Tetrachloroethene	298.15	1.614427	1.614320 [24]	1038.97	1032.1 (303.15 K) [10]	1.0305	1.030 [6]

2.2 Apparatus and Procedures

Before each series of measurements, the instrument was calibrated with triple-distilled freshly degassed water ($\rho = 997.075\,\text{kg}\cdot\text{m}^{-3}$) and dry air at atmospheric pressure. Densities of both water and dry air at the various working temperatures were supplied by the manufacturer in the instruction manual. The calibration was accepted if the measurements were within $2 \times 10^{-6}\,\text{g}\cdot\text{cm}^{-3}$ of the published values. The uncertainties were estimated to be within $2 \times 10^{-6}\,\text{g}\cdot\text{cm}^{-3}$. Air-tight stoppered bottles were used for the preparation of mixtures. The mass of the dry bottle was first determined. The less volatile component of the mixture was introduced in the bottle, and the total mass was measured. Subsequently, the other liquid component was introduced, and the mass of the bottle along with the two components was determined. All the mixtures were weighed on an electronic balance accurate to 0.1 mg. The average uncertainty in the mole fraction of the mixtures was estimated to be less than 1×10^{-4}. Conversion to molar quantities was based on the relative atomic mass table of 1985 issued by IUPAC [25]. From the results of densities and speeds of sound, the isentropic compressibility, κ_S was calculated as

$$\kappa_S = \frac{1}{u^2\rho} \tag{1}$$

The results of ρ and u compiled in Table 2 represent the average of at least three independent measurements for each composition of the mixture.

3 Results and Discussion

The excess molar volumes, V^{E}, of the solutions were calculated from the densities of the pure liquids and their mixtures using the following equation:

$$V^{\text{E}} = (x_1M_1 + x_2M_2)/\rho_{\text{mix}} - (x_1M_1/\rho_1 + x_2M_2/\rho_2) \tag{2}$$

where ρ_{mix} is the density of the mixture and x_1, M_1, ρ_1 and x_2, M_2, ρ_2 are the mole fraction, molar mass, and the density of pure components 1 and 2, respectively. The excess molar volumes were reproducible to $\pm 2 \times 10^{-3}\,\text{cm}^3\cdot\text{mol}^{-1}$. The first term in Eq. 2 represents the actual volume of the mixture, V_{mix}, and the second, the volume it would occupy if the mixture behaved ideally, V_{id}.

The following relations have been used to calculate the sound speed, u, of the binary liquid mixtures.

Nomoto's relation (NR) [26]:

$$u = \left(\frac{R_{\text{m}}}{V_{\text{mix}}}\right)^3 = \left(\frac{x_1R_1 + x_2R_2}{x_1V_1 + x_2V_2}\right)^3 \tag{3}$$

where x_1, x_2, V_1, V_2, and R_1, R_2 are mole fractions, molar volumes, and molar sound speeds of first and second components, respectively.

Table 2 Densities, ρ, ultrasonic speeds, u, isentropic compressibilities, κ_S, excess molar volumes, V^{E}, deviations of ultrasonic speeds, u^{D}, molar isentropic compressibilities, $\kappa_{S,\mathrm{m}}$, excess molar isentropic compressibilities, $\kappa_{S,\mathrm{m}}^{\mathrm{E}}$, and thermal expansion coefficients, α, for halohydrocarbons (1) + hexan-1-ol (2) at (293.15 and 298.15) K

x_1	ϕ_1	$\rho \times 10^{-3}$ $(\mathrm{kg \cdot m^{-3}})$	u $(\mathrm{m \cdot s^{-1}})$	κ_S $(\mathrm{TPa^{-1}})$	$V^{\mathrm{E}} \times 10^6$ $(\mathrm{m^3 \cdot mol^{-1}})$	u^{D} $(\mathrm{m \cdot s^{-1}})$	$\kappa_{S,\mathrm{m}} \times 10^{14}$ $(\mathrm{m^5 \cdot N^{-1} \cdot mol^{-1}})$	$\kappa_{S,\mathrm{m}}^{\mathrm{E}} \times 10^{14}$ $(\mathrm{m^5 \cdot N^{-1} \cdot mol^{-1}})$	$\alpha (kK)^{-1}$
1,2-Dichloroethane (1) + Hexan-1-ol (2) (293.15 K)									
0.0000	0.0000	0.818856	1320.11	700.76	0.000	0.00	8.74	0.000	0.8647
0.0370	0.0237	0.828769	1313.23	699.66	0.058	−1.21	8.62	0.024	0.8767
0.0769	0.0501	0.839847	1305.34	698.80	0.108	−3.06	8.48	0.055	0.8913
0.1499	0.1004	0.860583	1291.65	696.49	0.253	−5.48	8.23	0.104	0.9139
0.2147	0.1475	0.879725	1279.69	694.13	0.412	−7.36	8.01	0.148	0.9312
0.2935	0.2082	0.904954	1265.23	690.29	0.524	−10.16	7.72	0.193	0.9555
0.3952	0.2926	0.940475	1247.72	683.00	0.607	−13.36	7.33	0.235	1.0006
0.4532	0.3441	0.962107	1238.50	677.62	0.656	−14.67	7.09	0.252	1.0251
0.5596	0.4458	1.005050	1222.83	665.40	0.715	−16.75	6.65	0.271	1.0774
0.6113	0.4989	1.027551	1216.72	657.38	0.733	−16.74	6.41	0.266	1.0976
0.6971	0.5930	1.067981	1207.92	641.74	0.711	−16.57	6.00	0.250	1.1270
0.7791	0.6907	1.111055	1202.28	622.66	0.601	−15.53	5.59	0.214	1.1414
0.8563	0.7905	1.155161	1200.73	600.44	0.495	−12.41	5.17	0.163	1.1333
0.9335	0.8989	1.205426	1205.44	570.91	0.235	−6.27	4.70	0.075	1.1495
0.9790	0.9672	1.236986	1211.76	550.56	0.101	−0.29	4.41	0.013	1.1561
1.0000	1.0000	1.252766	1212.92	542.58	0.000	0.01	4.29	0.000	1.1373
1,2-Dichloroethane (1) + Hexan-1-ol (2) (298.15 K)									
0.0000	0.0000	0.815281	1303.19	722.23	0.000	0.00	9.05	0.000	0.8753
0.0370	0.0238	0.825105	1296.20	721.35	0.061	−1.29	8.92	0.026	0.8820
0.0769	0.0502	0.836074	1288.16	720.80	0.115	−3.25	8.79	0.061	0.8895

Table 2 continued

x_1	ϕ_1	$\rho \times 10^{-3}$ $(\mathrm{kg \cdot m^{-3}})$	u $(\mathrm{m \cdot s^{-1}})$	κ_S $(\mathrm{TPa^{-1}})$	$V^{\mathrm{E}} \times 10^6$ $(\mathrm{m^3 \cdot mol^{-1}})$	u^{D} $(\mathrm{m \cdot s^{-1}})$	$\kappa_{S,\mathrm{m}} \times 10^{14}$ $(\mathrm{m^5 \cdot N^{-1} \cdot mol^{-1}})$	$\kappa^{\mathrm{E}}_{S,\mathrm{m}} \times 10^{14}$ $(\mathrm{m^5 \cdot N^{-1} \cdot mol^{-1}})$	$\alpha (kK)^{-1}$
0.1499	0.1005	0.856620	1274.32	718.88	0.266	−5.75	8.53	0.114	0.9037
0.2147	0.1477	0.875586	1262.25	716.82	0.429	−7.66	8.31	0.161	0.9170
0.2935	0.2085	0.900591	1247.95	712.98	0.545	−10.21	8.01	0.206	0.9342
0.3952	0.2929	0.935784	1230.01	706.33	0.633	−13.69	7.62	0.254	0.9581
0.4532	0.3444	0.957223	1220.72	701.06	0.684	−14.98	7.38	0.271	0.9726
0.5596	0.4461	0.999790	1205.96	687.74	0.743	−16.55	6.91	0.285	1.0014
0.6113	0.4992	1.022091	1199.78	679.68	0.762	−16.59	6.67	0.281	1.0164
0.6971	0.5933	1.062138	1189.72	666.40	0.741	−16.74	6.26	0.268	1.0430
0.7791	0.6910	1.104851	1184.29	645.33	0.627	−15.23	5.82	0.226	1.0706
0.8563	0.7907	1.148594	1182.77	622.35	0.517	−11.79	5.39	0.169	1.0987
0.9335	0.8990	1.198465	1184.35	594.86	0.249	−8.40	4.92	0.098	1.1294
0.9790	0.9673	1.229798	1187.66	576.48	0.110	−3.25	4.63	0.038	1.1487
1.0000	1.0000	1.245555	1193.60	563.53	0.000	−0.01	4.48	0.000	1.1579
1,2-Dibromoethane (1) + Hexan-1-ol (2) (293.15 K)									
0.0000	0.0000	0.818856	1320.11	700.76	0.000	0.00	8.74	0.000	0.8647
0.0402	0.0281	0.856608	1296.69	694.30	0.073	0.59	8.56	0.002	0.8752
0.0682	0.0481	0.883413	1280.96	689.87	0.128	0.87	8.44	0.006	0.8801
0.1276	0.0918	0.941916	1249.37	680.15	0.229	1.31	8.17	0.014	0.8902
0.2056	0.1517	1.022358	1211.19	666.76	0.328	1.48	7.81	0.025	0.9035
0.2686	0.2023	1.090467	1182.94	655.33	0.391	1.46	7.52	0.033	0.9130
0.3892	0.3056	1.228973	1135.24	631.37	0.514	1.64	6.96	0.040	0.9339
0.4277	0.3405	1.276432	1121.20	623.21	0.484	1.23	6.78	0.045	0.9389
0.5444	0.4522	1.427131	1083.57	596.79	0.510	0.62	6.22	0.054	0.9496

Table 2 continued

x_1	ϕ_1	$\rho \times 10^{-3}$ $(\mathrm{kg \cdot m^{-3}})$	u $(\mathrm{m \cdot s^{-1}})$	κ_S $(\mathrm{TPa^{-1}})$	$V^{\mathrm{E}} \times 10^6$ $(\mathrm{m^3 \cdot mol^{-1}})$	u^{D} $(\mathrm{m \cdot s^{-1}})$	$\kappa_{S,\mathrm{m}} \times 10^{14}$ $(\mathrm{m^5 \cdot N^{-1} \cdot mol^{-1}})$	$\kappa_{S,\mathrm{m}}^{\mathrm{E}} \times 10^{14}$ $(\mathrm{m^5 \cdot N^{-1} \cdot mol^{-1}})$	$\alpha(kK)^{-1}$
0.6405	0.5517	1.561996	1057.41	572.58	0.486	−0.06	5.76	0.056	0.9609
0.7326	0.6543	1.701636	1036.51	547.00	0.426	−0.86	5.30	0.055	0.9673
0.8519	0.7989	1.899692	1016.83	509.12	0.304	−1.21	4.69	0.042	0.9707
0.9273	0.8981	2.036524	1009.94	481.41	0.191	−0.36	4.29	0.021	0.9670
0.9587	0.9413	2.096509	1008.30	469.16	0.134	0.05	4.12	0.012	0.9632
0.9782	0.9687	2.135291	1007.43	461.44	0.072	−0.07	4.02	0.007	0.9611
1.0000	1.0000	2.179591	1007.04	452.41	0.000	0.00	3.90	0.000	0.9577
1,2-Dibromoethane (1) + Hexan-1-ol (2) (298.15 K)									
0.0000	0.0000	0.815281	1303.19	722.23	0.000	0.00	9.05	0.000	0.8753
0.0402	0.0281	0.852830	1279.95	715.73	0.078	0.47	8.86	0.005	0.8778
0.0682	0.0481	0.879495	1264.36	711.25	0.135	0.68	8.74	0.010	0.8796
0.1276	0.0918	0.937690	1233.06	701.41	0.240	0.99	8.46	0.020	0.8834
0.2056	0.1517	1.017704	1195.28	687.76	0.344	1.07	8.10	0.033	0.8887
0.2686	0.2024	1.085450	1167.33	676.09	0.410	0.98	7.80	0.042	0.8932
0.3892	0.3057	1.223201	1120.21	651.48	0.539	1.31	7.22	0.053	0.9024
0.4277	0.3406	1.270414	1106.34	643.10	0.509	0.70	7.03	0.057	0.9055
0.5444	0.4523	1.420311	1069.22	615.86	0.535	0.10	6.45	0.065	0.9154
0.6405	0.5518	1.554455	1043.59	590.69	0.511	−0.39	5.97	0.065	0.9242
0.7326	0.6544	1.693371	1023.12	564.15	0.449	−1.04	5.50	0.062	0.9333
0.8519	0.7990	1.890444	1003.95	524.82	0.321	−1.14	4.86	0.045	0.9461
0.9273	0.8981	2.026658	997.38	496.02	0.200	−0.09	4.45	0.021	0.9549
0.9587	0.9413	2.086396	995.92	483.23	0.139	0.46	4.27	0.010	0.9587

Table 2 continued

x_1	ϕ_1	$\rho \times 10^{-3}$ $(\mathrm{kg \cdot m^{-3}})$	u $(\mathrm{m \cdot s^{-1}})$	κ_S $(\mathrm{TPa^{-1}})$	$V^{\mathrm{E}} \times 10^6$ $(\mathrm{m^3 \cdot mol^{-1}})$	u^{D} $(\mathrm{m \cdot s^{-1}})$	$\kappa_{S,\mathrm{m}} \times 10^{14}$ $(\mathrm{m^5 \cdot N^{-1} \cdot mol^{-1}})$	$\kappa^{\mathrm{E}}_{S,\mathrm{m}} \times 10^{14}$ $(\mathrm{m^5 \cdot N^{-1} \cdot mol^{-1}})$	$\alpha(kK)^{-1}$
0.9782	0.9688	2.125016	994.76	475.56	0.075	0.03	4.16	0.007	0.9611
1.0000	1.0000	2.169137	994.27	466.34	0.000	0.00	4.04	0.000	0.9639
1,1,2,2-Tetrachloroethene (1) + Hexan-1-ol (2) (293.15 K)									
0.0000	0.0000	0.818856	1320.11	700.76	0.000	0.00	8.74	0.000	0.8647
0.0688	0.0571	0.864637	1292.01	692.84	0.012	1.97	8.54	−0.024	0.8835
0.1230	0.1030	0.901521	1270.77	686.89	0.022	2.96	8.38	−0.036	0.8937
0.2457	0.2106	0.987759	1226.29	673.23	0.047	4.49	8.03	−0.053	0.9197
0.3618	0.3171	1.072992	1188.18	660.14	0.082	4.88	7.70	−0.053	0.9437
0.4502	0.4014	1.140457	1161.45	650.01	0.110	4.40	7.46	−0.042	0.9610
0.5583	0.5086	1.226302	1131.51	636.92	0.133	3.03	7.15	−0.021	0.9799
0.6518	0.6052	1.303622	1108.26	624.55	0.149	1.44	6.88	0.001	0.9940
0.7068	0.6638	1.350534	1095.82	616.62	0.156	0.40	6.72	0.014	1.0008
0.7419	0.7019	1.381185	1088.42	611.16	0.148	−0.32	6.61	0.022	1.0082
0.7797	0.7435	1.414647	1080.88	605.06	0.144	−1.11	6.49	0.031	1.0093
0.8315	0.8016	1.461437	1071.36	596.14	0.134	−2.22	6.33	0.042	1.0151
0.8718	0.8478	1.498800	1064.70	588.57	0.111	−3.11	6.19	0.049	1.0119
0.9179	0.9015	1.542246	1058.21	579.03	0.091	−3.74	6.03	0.053	1.0173
0.9504	0.9401	1.573609	1054.99	570.96	0.064	−3.42	5.90	0.045	1.0124
1.0000	1.0000	1.622745	1054.03	554.68	0.000	0.00	5.67	0.000	1.0222
1,1,2,2-Tetrachloroethene (1) + Hexan-1-ol (2) (298.15 K)									
0.0000	0.0000	0.815281	1303.19	722.23	0.000	0.00	9.05	0.000	0.8753
0.0688	0.0571	0.860792	1274.52	715.17	0.017	0.41	8.85	−0.003	0.8934

Table 2 continued

x_1	ϕ_1	$\rho \times 10^{-3}$ $(\text{kg} \cdot \text{m}^{-3})$	u $(\text{m} \cdot \text{s}^{-1})$	κ_S (TPa^{-1})	$V^{\text{E}} \times 10^6$ $(\text{m}^3 \cdot \text{mol}^{-1})$	u^{D} $(\text{m} \cdot \text{s}^{-1})$	$\kappa_{S,\text{m}} \times 10^{14}$ $(\text{m}^5 \cdot \text{N}^{-1} \cdot \text{mol}^{-1})$	$\kappa^{\text{E}}_{S,\text{m}} \times 10^{14}$ $(\text{m}^5 \cdot \text{N}^{-1} \cdot \text{mol}^{-1})$	$\alpha(kK)^{-1}$
0.1230	0.1031	0.897460	1253.65	708.98	0.029	1.05	8.69	−0.010	0.9050
0.2457	0.2107	0.983180	1209.55	695.22	0.061	1.58	8.33	−0.013	0.9315
0.3618	0.3172	1.067892	1171.56	682.25	0.100	1.09	8.00	−0.001	0.9552
0.4502	0.4016	1.134940	1144.91	672.18	0.130	0.14	7.75	0.016	0.9722
0.5583	0.5088	1.220256	1115.12	659.03	0.153	−1.47	7.44	0.040	0.9909
0.6518	0.6054	1.297102	1092.04	646.47	0.170	−2.94	7.16	0.060	1.0053
0.7068	0.6640	1.343732	1079.52	638.60	0.175	−3.95	6.99	0.073	1.0124
0.7419	0.7020	1.374186	1072.05	633.18	0.167	−4.60	6.88	0.080	1.0186
0.7797	0.7436	1.407460	1064.57	626.92	0.161	−5.13	6.76	0.085	1.0213
0.8315	0.8018	1.453969	1055.64	617.18	0.150	−5.26	6.58	0.083	1.0273
0.8718	0.8479	1.491149	1049.01	609.42	0.121	−5.72	6.44	0.084	1.0262
0.9179	0.9016	1.534331	1043.31	598.76	0.100	−4.98	6.27	0.071	1.0317
0.9504	0.9401	1.565562	1041.16	589.24	0.068	−3.11	6.12	0.044	1.0280
1.0000	1.0000	1.614427	1038.97	573.82	0.000	0.00	5.89	0.000	1.0305

Van Dael's ideal mixture relation (IMR) [27]:

$$\frac{1}{x_1M_1 + x_2M_2}\left(\frac{1}{u^2_{\mathrm{id,mix}}}\right) = \frac{x_1}{M_1u_1^2} + \frac{x_2}{M_2u_2^2} \tag{4}$$

where M_1, M_2 and u_1, u_2 are the molar masses and sound speeds of first and second components, respectively, and $u_{\mathrm{id,mix}}$ is the ultrasonic speed of the ideal mixture.

Jacobson's FLT [28]:

$$u_{\mathrm{mix}} = \frac{K}{L_{\mathrm{f(mix)}}\rho^{1/2}_{\mathrm{mix}}} \tag{5}$$

where K is Jacobson's constant that is temperature dependent only and its values are 618.0 and 625.0 at (293.15 and 298.15) K, respectively, $L_{\mathrm{f(mix)}}$ is the intermolecular free length of the binary mixture and ρ_{mix} is the density of the mixture.

$$L_{\mathrm{f}} = \frac{2V_{\mathrm{a}}}{Y} \tag{6}$$

where V_{a} represents the available volume per mole and Y is the surface area per mole and can be expressed as

$$V_{\mathrm{a}} = V_T - V_0 \tag{7}$$

$$Y = (36\pi N_{\mathrm{A}} V_0^2)^{1/3} \tag{8}$$

Here, N_{A} is the Avogadro number and V_0 and V_T are the molar volumes at 0 K and at temperature T, respectively. V_0 can be obtained from the following relation using the critical temperature T_{c}:

$$V_0 = V_T\,(1 - T/T_{\mathrm{c}})^{0.3} \tag{9}$$

The critical temperature of the studied systems is assumed to be the mole fraction average of the values of its pure components and is given by the relation,

$$T_{\mathrm{c}} = x_1T_{\mathrm{c1}} + x_2T_{\mathrm{c2}} \tag{10}$$

Assuming additivity of the surface area, the thermodynamic intermolecular free lengths in the binary liquid mixtures have been calculated using the relation,

$$L_{\mathrm{f}} = 2\left[V_T - \{x_1V_{0(1)} + x_2V_{0(2)}\}\right] / \,(x_1Y_1 + x_2Y_2) \tag{11}$$

The intermolecular free lengths, L_{f}, have also been computed using Eqs. 6 and 8 and Schaaffs' relation for available volume, V_{a},

$$V_{\mathrm{a}} = V_T[1 - (u/u_\infty)] \tag{12}$$

where u is the ultrasonic speed at temperature T and u_∞ is 1600 $\text{m} \cdot \text{s}^{-1}$. L_f obtained by this approach is known as the ultrasonic intermolecular free length.

Schaaffs' CFT [29–31]:

$$u_\text{mix} = u_\infty (x_1 S_1 + x_2 S_2) \frac{[(x_1 b_1 + x_2 b_2)]}{V_\text{mix}} \tag{13}$$

where b and S are the geometric volume and collision factor, respectively. The actual volume of the molecule per mole of the liquid has been computed using the relation,

$$b = \frac{4}{3}\pi r^3 N_\text{A} \tag{14}$$

where r is the molecular radius which has been computed using the relations,

$$b' = \left[\frac{M}{\rho} - \frac{\gamma RT}{\rho u^2}\left(\left(1 + \frac{Mu^2}{3\gamma RT}\right)^{1/2} - 1\right)\right] \tag{15}$$

$$r = \left(\frac{3b'}{16\pi N}\right)^{1/3} \tag{16}$$

where b' is the van der Waals constant and is equal to four times the actual volume of the molecules per mole of the liquid, i.e., $b' = 4b$ and $\gamma = C_P/C_V$ is the ratio of isobaric and isochoric heat capacities that can be obtained from the isentropic and isothermal compressibility coefficients, κ_S and κ_T, using the thermodynamic relation $\kappa_T/\kappa_S = C_P/C_V$. The value of the collision factor S has been calculated using the relation,

$$S = \frac{uV_T}{bu_\infty} \tag{17}$$

Junjie relation (JR) [32]:

$$u_\text{mix} = \frac{\sum_{i=1}^{2} x_i V_i}{\left(\sum_{i=1}^{2} x_i M_i\right)^{1/2} \cdot \left(\sum_{i=1}^{2} x_i M_i/\rho_i u_i^2\right)^{1/2}} \tag{18}$$

where x_i, M_i, ρ_i, and u_i are the mole fraction, molar mass, density, and ultrasonic speed, respectively, for component i.

Thermoacoustical approach [TAP] [33]:

The thermoacoustical method has also been employed to obtain the available volume, V_a, using the relation,

$$V_\text{a} = V_T\left(\frac{1}{K' + 1}\right) = V_T\left(\frac{1}{K'' + K + 1}\right) \tag{19}$$

where K', K, and K'' are known as the isothermal, isobaric, and isochoric acoustical parameters, respectively, and can be expressed by the relations,

$$K' = K + K'' = \frac{1}{2}\left[3 + \frac{S^*(1+\alpha T) + X}{\alpha T}\right] \tag{20}$$

$$K'' = 1 + X/(2\alpha T)$$

$$K = \frac{1}{2}\left[1 + \frac{S^*(1+\alpha T)}{\alpha T}\right] \tag{21}$$

$$S^* = 1 + \frac{4\alpha T}{3} \tag{22}$$

X is known as the isochoric temperature coefficient of the internal pressure and can be expressed as

$$X = 2\frac{(1+2\alpha T)}{\widetilde{V}^{C_1}} \tag{23}$$

where $\widetilde{V}$ represents the reduced molar volume and C_1 is the Moelwyn-Hughes parameter and can be expressed as

$$\widetilde{V} = \left[\frac{\alpha T/3}{1+\alpha T} + 1\right]^3 \tag{24}$$

$$C_1 = \frac{13}{3} + \frac{1}{\alpha T} + \frac{4\alpha T}{3} \tag{25}$$

The thermal expansion coefficient, α, has been calculated from the equation,

$$\alpha = (\partial V_{\text{mix}}/\partial T)_P / V_{\text{mix}} \tag{26}$$

The excess isentropic compressibilities, κ_S^{E}, were obtained from the relation [34],

$$\kappa_S^{\text{E}} = \kappa_S - \kappa_S^{\text{id}} \tag{27}$$

Here, the ideal isentropic compressibility term, κ_S^{id}, was computed using the relation,

$$\kappa_S^{\text{id}} = \sum_{i=1}^{2} \phi_i \left[\kappa_{S,i} + \frac{T V_i \left(\alpha_i^2\right)}{C_{P,i}}\right] - \left\{\frac{T\left(\sum_{i=1}^{2} x_i V_i\right)\left(\sum_{i=1}^{2} \phi_i \alpha_i\right)^2}{\sum_{i=1}^{2} x_i C_{P,i}}\right\} \tag{28}$$

where $C_{P,i}$ is the molar heat capacity of the ith component.

The volume fraction, ϕ_i, was calculated as

$$\phi_i = \frac{x_i V_i}{\sum_{i=1} x_i V_i} \tag{29}$$

The deviation of the speed of sound, u^{D}, from the speed of sound of an ideal mixture, is defined as [35]

$$u^{\mathrm{D}} = u - u^{\mathrm{id}} = u - \left(\rho^{\mathrm{id}}\kappa_S^{\mathrm{id}}\right)^{-1/2} \tag{30}$$

$$u^{\mathrm{id}} = \left(\rho^{\mathrm{id}}\kappa_S^{\mathrm{id}}\right)^{-1/2} \tag{31}$$

where u is the speed of sound of the mixture, $\rho^{\mathrm{id}} = \Sigma\phi_i\rho_i$ is the density of the corresponding ideal mixture, and ρ_i is the density of pure component i.

The product of the molar volume and the isentropic compressibility was calculated from the equation [35],

$$\kappa_{S,m} = VV^{-1}(\partial V/\partial P)_S = \mathrm{V}\kappa_S \tag{32}$$

where x_i and M_i are the mole fraction and molar mass of component i in the mixture. The corresponding excess molar isentropic compressibilities, $\kappa_{S,\mathrm{m}}^{\mathrm{E}}$, were obtained from the relation [36],

$$\kappa_{S,\mathrm{m}}^{\mathrm{E}} = \kappa_{S,\mathrm{m}} - \kappa_{S,\mathrm{m}}^{\mathrm{id}} \tag{33}$$

The values of ΔL_{f} have been calculated using the equation [5],

$$\Delta L_{\mathrm{f}} = L_{\mathrm{fmix}} - \left(L_{\mathrm{f}_1}x_1 + L_{\mathrm{f}_2}x_2\right) \tag{34}$$

The experimental results for V^{E}, u^{D}, $\kappa_{S,\mathrm{m}}^{\mathrm{E}}$, and α are presented in Table 2. The values of the acoustic parameters of pure components V, b', b, Y, S, γ, and V_0 used in and evaluated from the FLT and CFT formulations are listed in Table 3. The experimental results for r, L_{f}, V_{a}, and ΔL_{f} are given in Table 4 at (293.15 and 298.15) K. The percentage deviations (u (%)) were calculated using the relation,

$$u(\%) = \left(u_{\exp} - u_{\mathrm{calc}}\right) \times 100/u_{\exp} \tag{35}$$

where $u_{\exp}$ and u_{calc} are the experimental and calculated values of the ultrasonic speed, respectively. The standard percentage deviations (σ (%)) have also been calculated for each individual mixture, considering the percent deviations of the ultrasonic speed for all the mole fractions using the relation,

$$\sigma\ (\%) = \left[\sum (u(\%))^2 \,/\, (n-1)\right]^{1/2}, \tag{36}$$

where n represents the number of data points.

The plots of V^{E} with mole fraction x_1 for the binary mixtures of hexan-1-ol with 1,2-dichloroethane, 1,2-dibromoethane, and 1,1,2,2-tetrachloroethene at 293.15 K are depicted in Fig. 1. The V^{E} values are positive at all temperatures for these systems over the whole composition range. The excess molar volume, V^{E}, decreases

Table 3 Acoustic parameters for pure components at 298.15 K

Components	$V \times 10^6$ ($\mathrm{m^3 \cdot mol^{-1}}$)	$b' \times 10^6$ ($\mathrm{m^3 \cdot mol^{-1}}$)	$b \times 10^6$ ($\mathrm{m^3 \cdot mol^{-1}}$)	$Y \times 10^{-4}$ ($\mathrm{m^2 \cdot mol^{-1}}$)	S	γ	$V_0 \times 10^6$ ($\mathrm{m^3 \cdot mol^{-1}}$)
Hexan-1-ol	125.33	117.85	29.46	89.46	3.46	1.164	102.48
1,2-Dichloroethane	79.45	73.87	18.46	64.87	3.21	1.437	63.29
1,2-Dibromoethane	86.61	81.23	20.31	69.28	2.65	1.378	69.86
1,1,2,2-Tetrachloroethene	102.72	96.12	24.03	78.59	2.78	1.387	84.39

Table 4 Molecular radii, r, intermolecular free lengths, L_f, available volumes, V_a, and deviations of intermolecular free lengths, ΔL_f, for halohydrocarbons (1) + hexan-1-ol (2) at (293.15 and 298.15) K

x_1	r (Å)	L_f (FLT) (Å)	L_f (ultrasonic) (Å)	L_f (TAP) (Å)	$V_a \times 10^6$ (FLT) ($m^3 \cdot mol^{-1}$)	$V_a \times 10^6$ (ultrasonic) ($m^3 \cdot mol^{-1}$)	$V_a \times 10^6$ (TAP) ($m^3 \cdot mol^{-1}$)	ΔL_f (FLT) (Å)
1,2-Dichloroethane (1) + Hexan-1-ol (2) (293.15 K)								
0.0000	2.266	0.4974	0.4879	0.5925	22.25	21.83	26.51	0.0000
0.0370	2.256	0.4984	0.4984	0.5915	22.05	22.07	26.19	0.0015
0.0769	2.244	0.4992	0.5104	0.5903	21.82	22.35	25.85	0.0028
0.1499	2.224	0.5018	0.5309	0.5880	21.40	22.77	25.22	0.0064
0.2147	2.206	0.5050	0.5486	0.5858	21.04	23.09	24.66	0.0105
0.2935	2.182	0.5071	0.5691	0.5826	20.57	23.41	23.96	0.0136
0.3952	2.151	0.5084	0.5924	0.5783	19.95	23.62	23.06	0.0162
0.4532	2.133	0.5093	0.6040	0.5754	19.58	23.65	22.54	0.0178
0.5596	2.099	0.5100	0.6220	0.5698	18.90	23.54	21.57	0.0199
0.6113	2.082	0.5101	0.6277	0.5664	18.56	23.36	21.08	0.0207
0.6971	2.053	0.5089	0.6341	0.5603	17.98	22.93	20.26	0.0206
0.7791	2.024	0.5051	0.6344	0.5527	17.39	22.30	19.43	0.0179
0.8563	1.995	0.5012	0.6280	0.5450	16.84	21.48	18.64	0.0151
0.9335	1.965	0.4925	0.6101	0.5363	16.23	20.29	17.83	0.0074
0.9790	1.947	0.4878	0.5942	0.5309	15.88	19.43	17.36	0.0032
1.0000	1.939	0.4843	0.5892	0.5276	15.71	19.11	17.11	0.0000
1,2-Dichloroethane (1) + Hexan-1-ol (2) (298.15 K)								
0.0000	2.268	0.5108	0.5198	0.5968	22.84	23.25	26.69	0.0000
0.0370	2.258	0.5118	0.5305	0.5958	22.63	23.49	26.38	0.0014
0.0769	2.247	0.5126	0.5427	0.5946	22.40	23.76	26.03	0.0028

Table 4 continued

x_1	r (Å)	L_f (FLT) (Å)	L_f (ultrasonic) (Å)	L_f (TAP) (Å)	$V_a \times 10^6$ (FLT) ($m^3 \cdot mol^{-1}$)	$V_a \times 10^6$ (ultrasonic) ($m^3 \cdot mol^{-1}$)	$V_a \times 10^6$ (TAP) ($m^3 \cdot mol^{-1}$)	ΔL_f (FLT) (Å)
0.1499	2.227	0.5155	0.5635	0.5923	21.98	24.16	25.40	0.0066
0.2147	2.208	0.5188	0.5813	0.5902	21.60	24.47	24.84	0.0107
0.2935	2.185	0.5210	0.6015	0.5869	21.13	24.73	24.13	0.0140
0.3952	2.154	0.5225	0.6254	0.5820	20.49	24.93	23.20	0.0167
0.4532	2.136	0.5234	0.6370	0.5789	20.12	24.94	22.67	0.0184
0.5596	2.102	0.5243	0.6533	0.5726	19.42	24.73	21.67	0.0206
0.6113	2.085	0.5240	0.6589	0.5692	19.08	24.52	21.18	0.0210
0.6971	2.056	0.5237	0.6673	0.5632	18.48	24.13	20.36	0.0217
0.7791	2.027	0.5185	0.6665	0.5561	17.89	23.43	19.55	0.0176
0.8563	1.998	0.5156	0.6600	0.5489	17.31	22.57	18.77	0.0157
0.9335	1.968	0.5067	0.6465	0.5401	16.70	21.50	17.96	0.0078
0.9790	1.950	0.5018	0.6347	0.5347	16.34	20.75	17.48	0.0035
1.0000	1.941	0.4981	0.6222	0.5315	16.16	20.18	17.24	0.0000
1,2-Dibromoethane (1) + Hexan-1-ol (2) (293.15 K)								
0.0000	2.266	0.4974	0.4879	0.5925	22.25	21.83	26.51	0.0000
0.0370	2.257	0.4982	0.5272	0.5915	22.04	23.37	26.22	0.0019
0.0769	2.250	0.4989	0.5535	0.5906	21.89	24.38	26.02	0.0033
0.1499	2.237	0.5000	0.6056	0.5886	21.57	26.32	25.58	0.0060
0.2147	2.218	0.5006	0.6674	0.5857	21.15	28.47	24.99	0.0088
0.2935	2.203	0.5008	0.7120	0.5830	20.79	29.93	24.50	0.0106
0.3952	2.173	0.5011	0.7849	0.5775	20.11	32.03	23.57	0.0142
0.4532	2.163	0.4995	0.8051	0.5755	19.88	32.55	23.26	0.0137
0.5596	2.132	0.4974	0.8576	0.5689	19.19	33.66	22.33	0.0147

Table 4 continued

x_1	r (Å)	L_f (FLT) (Å)	L_f (ultrasonic) (Å)	L_f (TAP) (Å)	$V_a \times 10^6$ (FLT) ($m^3 \cdot mol^{-1}$)	$V_a \times 10^6$ (ultrasonic) ($m^3 \cdot mol^{-1}$)	$V_a \times 10^6$ (TAP) ($m^3 \cdot mol^{-1}$)	ΔL_f (FLT) (Å)
0.6113	2.107	0.4945	0.8908	0.5629	18.61	34.10	21.55	0.0144
0.6971	2.081	0.4905	0.9140	0.5564	18.04	34.14	20.78	0.0129
0.7791	2.046	0.4838	0.9298	0.5471	17.28	33.61	19.77	0.0094
0.8563	2.024	0.4783	0.9295	0.5403	16.79	32.89	19.12	0.0059
0.9335	2.014	0.4757	0.9271	0.5373	16.59	32.51	18.84	0.0042
0.9790	2.007	0.4732	0.9251	0.5353	16.45	32.26	18.67	0.0023
1.0000	2.000	0.4704	0.9218	0.5329	16.30	31.94	18.46	0.0000
1,2-Dibromoethane (1) + Hexan-1-ol (2) (298.15 K)								
0.0000	2.268	0.5107	0.5198	0.5968	22.84	23.25	26.692	0.0000
0.0370	2.259	0.5116	0.5590	0.5958	22.62	24.77	26.404	0.0020
0.0769	2.253	0.5123	0.5850	0.5949	22.47	25.76	26.197	0.0035
0.1499	2.239	0.5135	0.6368	0.5929	22.15	27.66	25.754	0.0062
0.2147	2.221	0.5142	0.6981	0.5899	21.71	29.77	25.160	0.0091
0.2935	2.205	0.5144	0.7423	0.5872	21.35	31.19	24.674	0.0110
0.3952	2.176	0.5149	0.8143	0.5818	20.65	33.22	23.740	0.0148
0.4532	2.165	0.5133	0.8343	0.5796	20.42	33.72	23.421	0.0142
0.5596	2.135	0.5112	0.8859	0.5729	19.71	34.76	22.480	0.0154
0.6113	2.109	0.5082	0.9182	0.5669	19.12	35.14	21.693	0.0150
0.6971	2.083	0.5041	0.9406	0.5603	18.53	35.12	20.923	0.0134
0.7791	2.049	0.4973	0.9553	0.5509	17.76	34.52	19.906	0.0098
0.8563	2.026	0.4915	0.9542	0.5441	17.25	33.75	19.247	0.0062
0.9335	2.016	0.4888	0.9514	0.5410	17.04	33.35	18.967	0.0043

Table 4 continued

x_1	r (Å)	L_f (FLT) (Å)	L_f (ultrasonic) (Å)	L_f (TAP) (Å)	$V_a \times 10^6$ (FLT) ($m^3 \cdot mol^{-1}$)	$V_a \times 10^6$ (ultrasonic) ($m^3 \cdot mol^{-1}$)	$V_a \times 10^6$ (TAP) ($m^3 \cdot mol^{-1}$)	ΔL_f (FLT) (Å)
0.9790	2.010	0.4863	0.9497	0.5389	16.90	33.11	18.788	0.0023
1.0000	2.003	0.4834	0.9464	0.5365	16.75	32.79	18.586	0.0000
1,1,2,2-Tetrachloroethene (1) + Hexan-1-ol (2) (293.15 K)								
0.0000	2.266	0.4975	0.4879	0.5925	22.25	21.83	26.51	0.0000
0.0370	2.256	0.4951	0.5347	0.5909	21.95	23.72	26.21	0.0006
0.0769	2.249	0.4932	0.5698	0.5898	21.71	25.11	25.99	0.0010
0.1499	2.232	0.4889	0.6420	0.5867	21.16	27.86	25.46	0.0020
0.2147	2.215	0.4851	0.7023	0.5833	20.65	30.03	24.94	0.0031
0.2935	2.202	0.4820	0.7437	0.5812	20.27	31.44	24.57	0.0039
0.3952	2.186	0.4780	0.7887	0.5789	19.79	32.88	24.14	0.0045
0.4532	2.173	0.4743	0.8225	0.5761	19.39	33.87	23.72	0.0049
0.5596	2.164	0.4720	0.8400	0.5756	19.15	34.34	23.53	0.0050
0.6113	2.159	0.4702	0.8500	0.5746	18.99	34.59	23.38	0.0047
0.6971	2.153	0.4684	0.8601	0.5740	18.83	34.82	23.24	0.0045
0.7791	2.144	0.4658	0.8723	0.5718	18.60	35.07	22.99	0.0041
0.8563	2.138	0.4633	0.8803	0.5699	18.42	35.20	22.78	0.0034
0.9335	2.130	0.4606	0.8876	0.5681	18.22	35.26	22.57	0.0027
0.9790	2.125	0.4584	0.8904	0.5667	18.07	35.21	22.41	0.0019
1.0000	2.117	0.4544	0.8878	0.5636	17.85	34.87	22.14	0.0000
1,1,2,2-Tetrachloroethene (1) + Hexan-1-ol (2) (298.15 K)								
0.0000	2.268	0.5107	0.5198	0.5968	22.84	23.25	26.69	0.0000
0.0370	2.259	0.5084	0.5678	0.5955	22.53	25.18	26.41	0.0007
0.0769	2.251	0.5065	0.6022	0.5942	22.28	26.53	26.18	0.0013

Table 4 continued

x_1	r (Å)	L_f (FLT) (Å)	L_f (ultrasonic) (Å)	L_f (TAP) (Å)	$V_a \times 10^6$ (FLT) ($m^3 \cdot mol^{-1}$)	$V_a \times 10^6$ (ultrasonic) ($m^3 \cdot mol^{-1}$)	$V_a \times 10^6$ (TAP) ($m^3 \cdot mol^{-1}$)	ΔL_f (FLT) (Å)
0.1499	2.234	0.5023	0.6739	0.5911	21.73	29.24	25.65	0.0024
0.2147	2.218	0.4983	0.7342	0.5880	21.21	31.40	25.14	0.0036
0.2935	2.205	0.4953	0.7755	0.5855	20.81	32.79	24.75	0.0045
0.3952	2.189	0.4911	0.8203	0.5820	20.33	34.20	24.27	0.0051
0.4532	2.175	0.4873	0.8538	0.5788	19.91	35.16	23.84	0.0054
0.5596	2.167	0.4849	0.8714	0.5768	19.66	35.63	23.58	0.0055
0.6113	2.161	0.4831	0.8815	0.5755	19.51	35.87	23.42	0.0052
0.6971	2.155	0.4812	0.8915	0.5739	19.34	36.10	23.24	0.0050
0.7791	2.147	0.4785	0.9027	0.5718	19.10	36.29	22.99	0.0045
0.8563	2.140	0.4759	0.9106	0.5699	18.92	36.41	22.79	0.0037
0.9335	2.133	0.4731	0.9165	0.5679	18.71	36.42	22.57	0.0030
0.9790	2.127	0.4707	0.9174	0.5661	18.56	36.29	22.40	0.0020
1.0000	2.119	0.4665	0.9166	0.5636	18.33	36.02	22.14	0.0000

in the sequence: 1,2-dichloroethane + hexan-1-ol $>$ 1,2-dibromoethane + hexan-1-ol $>$ 1,1,2,2-tetrachloroethene+hexan-1-ol. The maximum in the V^{E} curves in the case of the 1,2-DCE + hexan-1-ol system agrees with the value reported for this system at 303.15 K [13]. A similar type of behavior has been observed for the variation of V^{E} with mole fraction for the binary mixtures of 1,2-dichloroethane + heptanol and 1,1,2,2-tetrachloroethane + heptanol [6]. The magnitude of the maximum value of V^{E} increases slightly with an increase of temperature from 293.15 K to 298.15 K.

The sign and magnitude of V^{E} varies with the structural characteristics of the components arising from the geometrical fitting of one component into the structure of the other component because of the differences in the size, shape, and nature of the components and the free volume. Since the molar volumes of hexan-1-ol ($125.33 \times 10^{-6}\,\mathrm{m^3 \cdot mol^{-1}}$), 1,2-dichloroethane ($79.45 \times 10^{-6}\,\mathrm{m^3 \cdot mol^{-1}}$), 1,2-dibromoethane ($86.61 \times 10^{-6}\,\mathrm{m^3 \cdot mol^{-1}}$), and 1,1,2,2-tetrachloroethene ($102.72 \times 10^{-6}\,\mathrm{m^3 \cdot mol^{-1}}$) at 298.15 K differ considerably, it seems that the halogenated hydrocarbon molecules intercalate between the polymeric entities of hexan-1-ol and disrupt their H-bonding. Consequently, there is an increase in the total volume of the solution. The destruction of short-range orientation structural order present in pure liquids, viz., H-bonds in hexan-1-ol and dipolar interactions in halogenated hydrocarbons makes V^{E} positive since the aggregates have smaller volumes than the sum of their individual components [12]. Due to the presence of four chlorine atoms in 1,1,2,2-TCE as compared to two in 1,2-DCE and two bromine atoms in 1,2-DBE, four H-bonds of the type Cl$\cdots$H–O may be formed between the OH group of hexan-1-ol polymeric entities and the 1,1,2,2-TCE molecule as compared to two Cl$\cdots$H–O bonds in 1,2-DCE+hexan-1-ol and two Br$\cdots$H–O bonds in the 1,2-DBE + hexan-1-ol system. The unsaturation present in 1,1,2,2-TCE will also contribute towards the interaction strength of 1,1,2,2-TCE + hexan-1-ol and may be involved in the formation of the OH$\cdots\pi$ electron H-bonded complex which may lead to a decrease in the molar excess volume V^{E} [6–8]. The new possible H-bond interactions of the type Cl$\cdots$H–O and Br$\cdots$H–O, and π-bond interactions of the type O–H$\cdots\pi$, and weak physical intermolecular interactions in the 1,1,2,2-tetrachloroethene + hexan-1-ol system are weaker than the dipolar interactions in pure halogenated hydrocarbons and H-bonding in hexan-1-ol. Since the structure-breaking effect and the effects of interactions between like and unlike molecules balance each other to different degrees [13–19] in the 1,1,2,2-tetrachloroethene and hexan-1-ol mixtures, there is only a small increase in V^{E} values in this case.

The curves for the deviations of the ultrasonic speed, u^{D}, versus x_1 at 293.15 K for the studied systems are presented in Fig. 2, and their variations are of a quite different nature than those of the molar excess volumes, V^{E}. The u^{D} values are negative over the whole composition range for the 1,2-DCE + hexan-1-ol system whereas sigmoidal trends are observed for the 1,2-DBE + hexan-1-ol and 1,1,2,2-TCE + hexan-1-ol systems. The negative values at the minimum of these curves vary in the order: $u^{\mathrm{D}}_{\text{DCE-HEX}} > u^{\mathrm{D}}_{\text{TCE-HEX}} > u^{\mathrm{D}}_{\text{DBE-HEX}}$.

The results for excess molar isentropic compressibilities, $\kappa^{\mathrm{E}}_{S,\mathrm{m}}$, versus x_1 at 293.15 K are presented in Fig. 3. The $\kappa^{\mathrm{E}}_{S,\mathrm{m}}$ values are positive over the whole composition range for the binary mixtures of 1,2-DCE + hexan-1-ol and 1,2-DBE + hexan-1-ol, whereas a sigmoidal trend is observed for the 1,1,2,2-TCE + hexan-1-ol system. The

Fig. 1 Excess molar volumes, V^{E}, versus mole fraction, x_1, at 293.15 K for binary mixtures of hexan-1-ol with (■) 1,2-dichloroethane, (○) 1,2-dibromoethane, and (▲) 1,1,2,2-tetrachloroethene

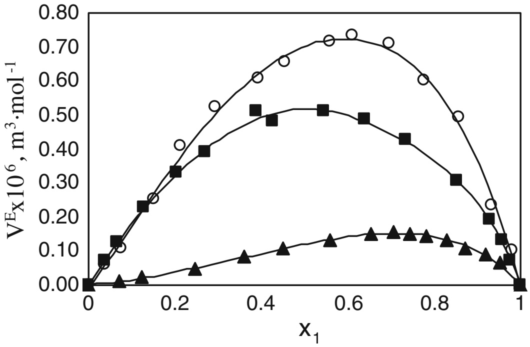

Fig. 2 Deviations of ultrasonic speeds, u^{D}, versus mole fraction, x_1, at 293.15 K for binary mixtures of hexan-1-ol with (■) 1,2-dichloroethane, (○) 1,2-dibromoethane, and (▲) 1,1,2,2-tetrachloroethene

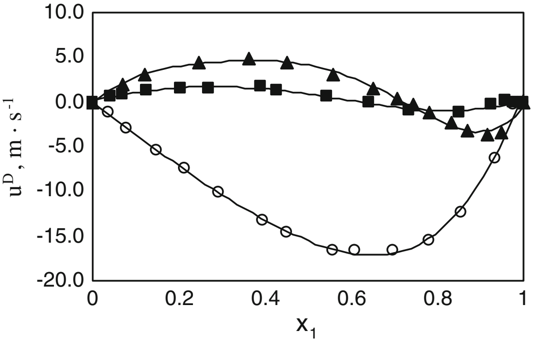

$\kappa^{\mathrm{E}}_{S,\mathrm{m}}$ values are negative in the low mole fraction region for 1,1,2,2-TCE up to $x_1 \approx 0.65$ and become more positive with an increase in the mole fraction of 1,1,2,2-TCE. The positive values at the maximum of these curves vary in the order: $\kappa^{\mathrm{E}}_{S,\mathrm{mDBE\text{-}HEX}} < \kappa^{\mathrm{E}}_{S,\mathrm{mTCE\text{-}HEX}} < \kappa^{\mathrm{E}}_{S,\mathrm{mDCE\text{-}HEX}}$ and the $\kappa^{\mathrm{E}}_{S,\mathrm{m}}$ values become more positive with an increase of temperature. The overall behavior of $\kappa^{\mathrm{E}}_{S,\mathrm{m}}$ is similar to that of u^{D} (Fig. 2) for all the binary mixtures but is of the opposite sign [37]. A similar trend has been observed for 1,2-DCE + octan-1-ol and 1,1,2,2-tetrachloroethane + octan-1-ol systems [5]. The positive values of $\kappa^{\mathrm{E}}_{S,\mathrm{m}}$ imply a higher compressibility of the binary liquid mixtures than the corresponding ideal mixtures. Therefore, in these systems, an expansion in free volume occurs, making the mixtures more compressible than the ideal mixtures which ultimately culminates in the positive values of $\kappa^{\mathrm{E}}_{S,\mathrm{m}}$ leading to weaker intermolecular interactions.

The intermolecular free length, L_{f}, computed using the FLT and Schaafs' CFT, increases with an increase in the mole fraction of these halohydrocarbons except in the case of the 1,1,2,2-tetrachloroethene + hexan-1-ol system where the FLT predicts that L_{f} decreases with an increase in the mole fraction of 1,1,2,2-tetrachloroethene (Fig. 4). The change in the slope of the isotherms of L_{f} as a function of the mole fraction in the higher mole fraction region of 1,2-dibromoethane and 1,2-dichloroethane predicted by these theories shows that the entropy effect related to the structural rearrangement of solvent molecules [38,39] caused mainly by the disruption of the

Fig. 3 Excess molar isentropic compressibilities, $\kappa^{\mathrm{E}}_{S,\mathrm{m}}$, versus mole fraction, x_1, at 293.15 K for binary mixtures of hexan-1-ol with (■) 1,2-dichloroethane, (◯) 1,2-dibromoethane, and (▲) 1,1,2,2-tetrachloroethene

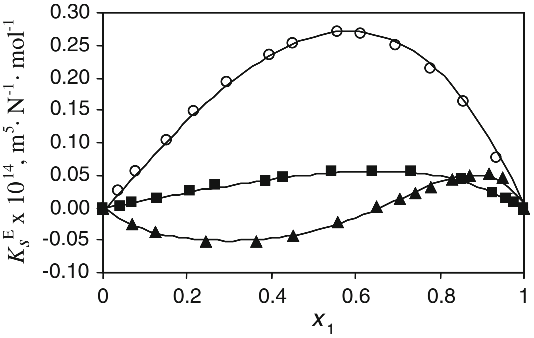

Fig. 4 Intermolecular free lengths, L_{f}, versus mole fraction, x_1, at 293.15 K for binary mixtures of hexan-1-ol with (■) 1,2-dichloroethane, (◯) 1,2-dibromoethane, and (▲) 1,1,2,2-tetrachloroethene obtained using (i) FLT, (ii) CFT, and (iii) TAP formulations

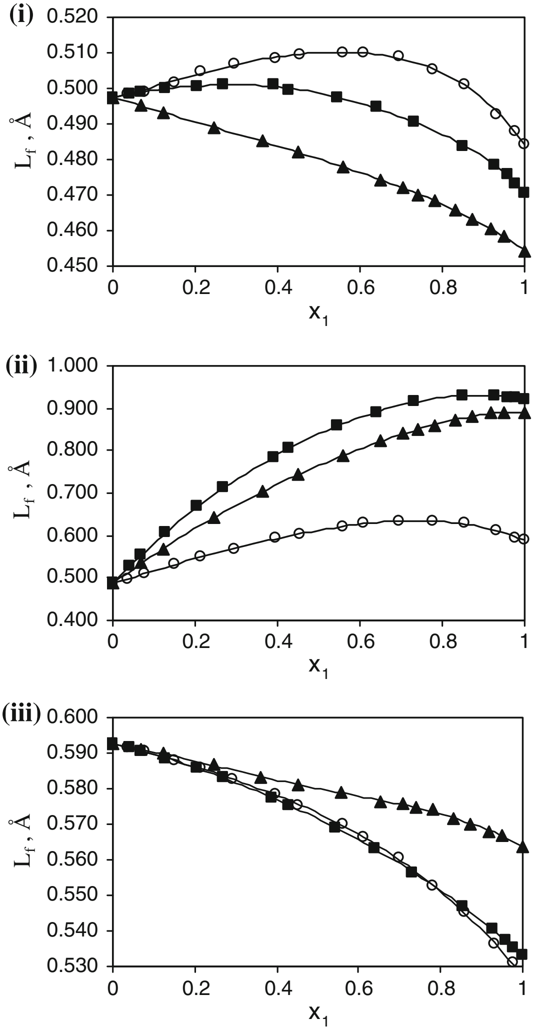

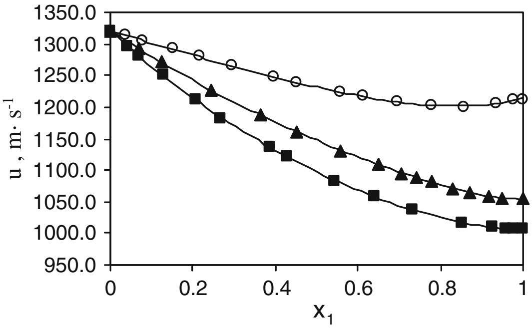

Fig. 5 Ultrasonic velocities, u, versus mole fraction, x_1, at 293.15 K for binary mixtures of hexan-1-ol with (■) 1,2-dichloroethane, (○) 1,2-dibromoethane, and (▲) 1,1,2,2-tetrachloroethene

hexan-1-ol multimers occurs in these two systems. However, the mixing process is accompanied by a decrease in the intermolecular free length, L_f, in the binary mixture of the hexan-1-ol + 1,1,2,2-tetrachloroethene system on an increase in the mole fraction of this halohydrocarbon (Fig. 4), presumably because of the combined effect of self-association and solvation processes associated with the disruption of long-chain polymeric entities of hexan-1-ol on the successive addition of 1,1,2,2-tetrachloroethene. The thermoacoustic approach (TAP), however, predicts that the intermolecular free length, L_f, in these binary mixtures decreases with an increase in the mole fraction of these halohydrocarbons. The L_f values for the pure components vary in the order:

$L_{\mathrm{f(DCE)}} > L_{\mathrm{f(DBE)}} > L_{\mathrm{f(TCE)}}$ (FLT)
$L_{\mathrm{f(DBE)}} > L_{\mathrm{f(TCE)}} > L_{\mathrm{f(DCE)}}$ (CFT)
$L_{f(TCE)} > L_{\mathrm{f(DBE)}} > L_{\mathrm{f(DCE)}}$ (TAP)

The values of L_f for all three binary mixtures obtained from the ultrasonic method are higher than the values computed from the thermodynamic and thermoacoustical methods [40] (Table 4). This trend has also been observed for the binary liquid mixtures of 1,1,2,2-tetrachloroethane with benzene, toluene, paraxylene, acetone, cyclohexane [40], and liquid methane with liquid tetrafluoromethane [41], and the other multicomponent liquid mixtures [42]. The thermodynamic method [42] has been found to be better than the ultrasonic method for calculating L_f values provided T is not very close to T_c because the right-hand side of Eq. 9 vanishes when $T > T_\mathrm{c}$. On the other hand, the ultrasonic method fails completely when the sound speed of the liquid or their mixtures exceeds $1600\,\mathrm{m \cdot s^{-1}}$ since the right-hand side of Eq. 12 disappears when $u > u_\infty$.

The variation of the ultrasonic speed, u, for a mixture depends on the increase or decrease in the values of L_f and on the temperature. In general, u and L_f vary in a reciprocal manner with the mole fraction, x_1, of a mixture [43,44]. A perusal of Table 2 reveals that the values of u decrease with an increase in x_1 of halohydrocarbons for all the binary mixtures under consideration (Fig. 5). However, the value of u starts increasing with an increase in x_1 of 1,2-dichloroethane above $x_1 \approx 0.86$ in the case of the 1,2-dichloroethane + hexan-1-ol mixture. The increase in the value of L_f with x_1 of a mixture with a corresponding decrease in u, predicted best on the basis of CFT

Fig. 6 Available volumes , V_a, versus mole fraction, x_1, at 293.15 K for binary mixtures of hexan-1-ol with (■) 1,2-dichloroethane, (○) 1,2-dibromoethane, and (▲) 1,1,2,2-tetrachloroethene obtained using (i) FLT, (ii) CFT, and (iii) TAP formulations

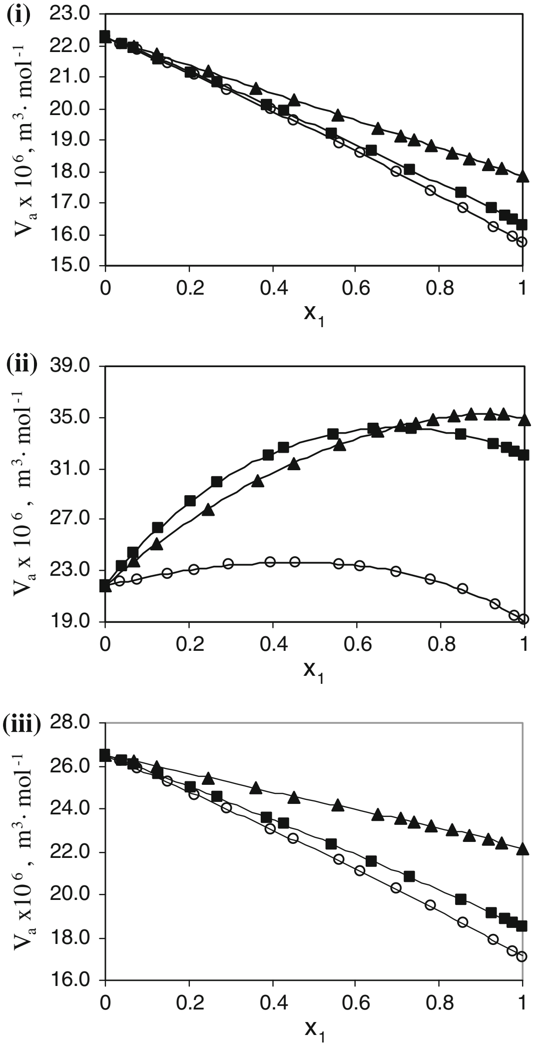

formulations, again supports weak molecular interactions taking place between the component molecules in the case of all the binary mixtures. The reciprocal relationship between u and L_f is not strictly observed on the basis of TAP and FLT formulations. With an increase in temperature, the density decreases and the gap between the molecules increases due to the increase in the molar free volume. A wider gap between the molecules is the main reason for the impediment to the propagation of ultrasonic waves, and consequently, the ultrasonic speed decreases with an increase in the temperature.

The available volume, V_a, computed using FLT and TAP, decreases with an increase in the mole fraction of halohydrocarbons for all the systems under consideration, but

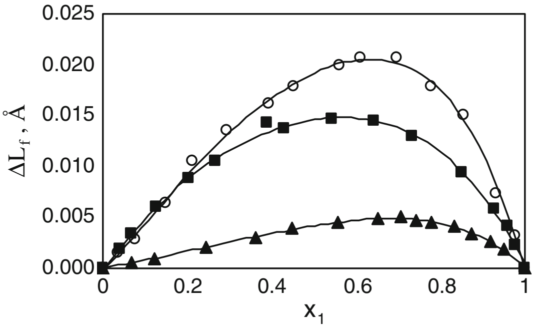

Fig. 7 Deviations of intermolecular free lengths, ΔL_{f}, versus mole fraction, x_1, at 293.15 K for binary mixtures of hexan-1-ol with (■) 1,2-dichloroethane, (○) 1,2-dibromoethane, and (▲) 1,1,2,2-tetrachloroethene

the CFT formulations predict that the available volume, V_{a}, increases with an increase in the mole fraction of halohydrocarbons and starts decreasing in the higher mole fraction region for all the studied systems (Fig. 6). The variations of excess functions, V^{E}, with mole fraction for these systems are consistent with the following order of molecular radii of the pure components (Table 4): $r_{\mathrm{DCE}} < r_{\mathrm{DBE}} < r_{\mathrm{TCE}} < r_{\mathrm{HEX}}$. The larger is the molecular radius, the greater is the structure-breaking effect on the self-associated hexan-1-ol, and the smaller will be the values of the deviation functions ΔL_{f} [5] and the higher will be the strength of specific interactions between hexan-1-ol and the halohydrocarbon molecule. The values of ΔL_{f} at the maximum of the curves (Fig. 7) are in the following order: $\Delta L_{\mathrm{fDCE\text{-}Hex}} > \Delta L_{\mathrm{fDBE\text{-}Hex}} > \Delta L_{\mathrm{fTCE\text{-}Hex}}$.

The minimum values of ΔL_{f} are consistent with the observation of the minimum excess molar volume, V^{E}, of the binary mixtures of the 1,1,2,2-tetrachloroethene + hexan-1-ol system due to specific intermolecular interactions resulting in the formation of molecular complexes. The increase in the excess molar volume, V^{E}, the negative deviation in sound speed, u^{D}, and the positive excess isentropic compressibility, $\kappa^{\mathrm{E}}_{S,\mathrm{m}}$, support the main factor of gradual disruption of the self-associated hexan-1-ol molecules on the addition of the halohydrocarbons and the weak physical intermolecular interactions [9,32,45,46] and the relatively weaker interactions of the type Cl···H–O and Br···H–O and π-bond interactions of the type O–H···π between unlike molecules. For the pure components, the values of V, b, and r show the same relations: hexan-1-ol > 1,1,2,2-tetrachloroethene > 1,2-dibromoethane > 1,2-dichloroethane. This observation is consistent with the trend observed for V^{E}, $\kappa^{\mathrm{E}}_{S,\mathrm{m}}$, and ΔL_{f} data for these systems.

A close examination of Table 4 clearly illustrates reasonably good agreement in the values of the intermolecular free lengths computed from the thermodynamic, ultrasonic, and thermoacoustic methods. The credibility of the results is further increased by the small standard percentage deviations (σ (%)) of ultrasonic speeds in Table 5 obtained using Nomoto's relation (NR) [26], Van Dael's ideal mixture relation (IMR) [27], Jacobson's FLT [28], and Schaaffs' CFT [29–31] for all the systems under consideration. An analysis of the standard percentage deviations (σ (%)) presented in Table 5 reveals that the results for the ultrasonic speeds for the 1,2-dibromoroethane + hexan-1-ol and 1,1,2,2-tetrachloroethene + hexan-1-ol systems can be satisfactorily explained by Van Dael ideal mixture relations (minimum σ (%) $= 1.89$ % and 1.25 %,

Table 5 Average percentage deviations, APD, and standard percentage deviations, σ (%), calculated by Nomoto (N), Van Dael (VD), free length theory (FLT), collision factor theory (CFT), and Junjie theory (J) for halohydrocarbons (1) + hexan-1-ol (2) at (293.15 and 298.15) K

System	T (K)	APD values					σ (%) values				
		$(\mathrm{APD})_{\mathrm{N}}$	$(\mathrm{APD})_{\mathrm{VD}}$	$(\mathrm{APD})_{\mathrm{FLT}}$	$(\mathrm{APD})_{\mathrm{CFT}}$	$(\mathrm{APD})_{\mathrm{J}}$	$(\sigma\ (\%))_{\mathrm{N}}$	$(\sigma\ (\%))_{\mathrm{VD}}$	$(\sigma\ (\%))_{\mathrm{FLT}}$	$(\sigma\ (\%))_{\mathrm{CFT}}$	$(\sigma\ (\%))_{\mathrm{J}}$
1,2-DCE (1) + Hexan-1-ol (2)	293.15	−2.13	−1.42	−0.33	−1.27	−2.26	2.87	1.95	3.43	1.73	7.69
	298.15	−2.17	−1.65	−0.454	−1.47	−2.55	2.90	1.94	3.35	1.72	7.75
1,2-DBE (1) + Hexan-1-ol (2)	293.15	−4.02	−1.37	2.93	−2.79	10.75	5.49	1.89	6.44	3.80	19.14
	298.15	−4.04	−1.39	2.95	−2.79	10.53	5.53	1.92	6.28	3.82	19.05
1,1,2,2-TCE (1) + Hexan-1-ol (2)	293.15	−2.59	−0.98	−3.38	−2.09	7.85	3.27	1.25	3.57	2.63	13.16
	298.15	−2.64	−1.03	−3.54	−2.13	7.59	3.35	1.32	3.73	2.70	13.01

respectively, for these systems at 293.15 K). However, the prediction of these results is better for the 1,2-dichloroethane + hexan-1-ol system by the CFT formulations (minimum σ (%) $= 1.73\,\%$ at 293.15 K). The Junjie relation (JR) gives higher σ (%) values for all the systems under consideration (minimum σ (%) $= 7.69\,\%$, $19.14\,\%$, and $13.16\,\%$ for the hexan-1-ol with DCE, DBE, and TCE systems, respectively, at 293.15 K).

4 Conclusion

In this paper, the densities and ultrasonic speeds of binary mixtures of hexan-1-ol with 1,2-dichloroethane, 1,2-dibromoethane, and 1,1,2,2-tetrachloroethene have been measured over the entire range of composition at (293.15 and 298.15) K, and good accordance has been found between the experimental and literature values. The observed positive values of V^{E} in conjunction with the $\kappa^{\mathrm{E}}_{S,\mathrm{m}}$ and ΔL_{f} data over the entire composition range for the studied mixtures confirm that the H-bond interactions of the type Cl$\cdots$H–O and Br$\cdots$H–O, and $\pi\cdots$H and/or weak physical intermolecular interactions between hexan-1-ol and the halohydrocarbon molecules dominate over the structure-breaking effect of hexan-1-ol on the addition of halohydrocarbons.

Acknowledgment Authors are grateful to the Kurukshetra University authorities for providing the necessary facilities to carry out the research work.

References

1. S.C. Bhatia, N. Tripathi, G.P. Dubey, Indian J. Pure Appl. Phys. **39**, 776 (2001)
2. S.C. Bhatia, N. Tripathi, G.P. Dubey, Indian J. Chem. **41A**, 266 (2002)
3. S.C. Bhatia, N. Tripathi, G.P. Dubey, Indian J. Pure Appl. Phys. **43**, 175 (2005)
4. S.C. Bhatia, R. Bhatia, G.P. Dubey, J. Chem. Eng. Data **54**, 3303 (2009)
5. S.C. Bhatia, R. Bhatia, G.P. Dubey, Phys. Chem. Liq. **48**(2), 199 (2009)
6. H. Iloukhani, B. Samiety, J. Chem. Eng. Data **50**, 1911 (2005)
7. M. Hasan, U.B. Kadam, A.P. Hiray, A.B. Sawant, J. Chem. Eng. Data **51**, 60 (2006)
8. M. Hasan, U.B. Kadam, A.P. Hiray, A.B. Sawant, J. Chem. Eng. Data **51**, 671 (2006)
9. M. Hasan, U.B. Kadam, A.P. Hiray, A.B. Sawant, J. Chem. Eng. Data **51**, 1797 (2006)
10. H. Iloukhani, M.V.P. Rao, Phys. Chem. Liq. **15**, 137 (1985)
11. P.S. Nikam, T.R. Mahale, M. Hasan, Acust. Acta Acust. **84**, 579 (1998)
12. R.D. Peralta, R. Infante, G. Cortez, A. Cisneros, Chem. Eng. Commun. **192**, 684 (2005)
13. N.V. Choudary, P.R. Naidu, Can. J. Chem. **59**(14), 2210 (1981)
14. M. Chorazewski, J. Chem. Eng. Data **52**, 154 (2007)
15. N.V. Choudary, A. Krishnaiah, P.R. Naidu, J. Chem. Eng. Data **27**, 412 (1982)
16. N.V. Choudary, J.C. Mouli, P.R. Naidu, Acoust. Lett. **6**, 56 (1982)
17. S.L. Oswal, I.N. Patel, J. Mol. Liq. **116**, 99 (2005)
18. A. Ali, A.K. Nain, D. Chand, R. Ahmad, Phys. Chem. Liq. **43**, 205 (2005)
19. G. Larsen, Z.K. Ismal, B. Herreies, R.D. Perra, J. Phys. Chem. **102**, 4734 (1998)
20. A.S. Al-Jimaj, J.A. Al-Kandery, A.M. Abdul-Latif, J. Chem. Eng. Data **52**, 216 (2007)
21. M. Dzida, J. Chem. Eng. Data **52**, 521 (2007)
22. T.M. Aminabhavi, V.B. Patil, J. Chem. Eng. Data **43**, 497 (1998)
23. J. Nath, Fluid Phase Equilib. **11**, 261 (2002)
24. J.A. Riddick, W.B. Bunger, T.K. Sakano, *Organic Solvents, Physical Properties and Methods of Purification*, vol. II, 4th edn. (Wiley Interscience, New York, 1986)
25. Commission on Atomic Weights and Isotopic Abundances 1985, Pure Appl. Chem. **58**, 1677 (1986)
26. O. Nomoto, J. Phys. Soc. Jpn. **13**, 1528 (1958)

27. W. Van Dael, *Thermodynamic Properties and Speed of Sound*, Chap. 5 (Butterworths, London, 1975)
28. B. Jacobson, Acta Chem. Scand. A **6**, 1485 (1952)
29. W. Schaaffs, Acoustica **33**, 272 (1975)
30. W. Schaaffs, *Molekularakustik*, Chaps. 11, 12 (Springer-Verlag, Berlin, 1963)
31. R. Nutsch-Kuhnkies, Acoustica **15**, 383 (1965)
32. Z. Junjie, J. Chem. Univ. Sci. Technol. **14**, 298 (1984)
33. A. Ali, A.K. Nain, Pramana-J. Phys. **58**, 695 (2002)
34. O. Kiyohara, G.C. Bensen, J. Chem. Thermodyn. **11**, 861 (1979)
35. A. Pal, R.K. Bhardwaj, Z. Phys. Chem. **216**, 1033 (2002)
36. K. Bebek, A. Strugala, Mol. Quant. Acoust. **27**, 337 (2006)
37. R.J. Fort, W.R. Moore, Trans. Faraday Soc. **61**, 2102 (1965)
38. K. Bebek, G. Filosek, S. Earnst, Mol. Quant. Acoust. **25**, 23 (2004)
39. K. Bebek, Mol. Quant. Acoust. **26**, 15 (2005)
40. J.D. Pandey, G.P. Dubey, B.P. Shukla, S.N. Dubey, J. Phys. **37**, 497 (1991)
41. J.D. Pandey, S.N. Srivastav, Acustica **51**, 66 (1982)
42. J.D. Pandey, R. Dey, J. Chhabra, Phys. Chem. Commun. **6**, 55 (2003)
43. A. Ali, A.K. Nain, M. Kamil, Thermochim. Acta **274**, 209 (1996)
44. A. Ali, S. Hyder, A.K. Nain, J. Mol. Liq. **79**, 89 (1999)
45. C. Yang, H. Lai, Z. Liu, P. Ma, J. Chem. Eng. Data **51**, 1345 (2006)
46. T.M. Aminabhavi, K. Banerjee, J. Chem. Eng. Data **43**, 509 (1998)